Linear theory of electron temperature anisotropy instabilities: Whistler, mirror, and Weibel

S. Peter Gary
Los Alamos National Laboratory
Los Alamos, NM
and
Homa Karimabadi
Department of Electrical and Computer Engineering
University of California, San Diego
La Jolla, CA

4 April 2006

Abstract

A collisionless, homogeneous plasma in which the electron velocity distribution is a bi-Maxwellian with $T_\perp > T_\parallel$, where the subscripts refer to directions relative to the background magnetic field $\mathbf{B}_o$, can support the growth of two distinct instabilities. Linear dispersion theory predicts that the whistler anisotropy instability is excited with maximum growth rate γ_m at $\mathbf{k} \times \mathbf{B}_o = 0$ and real frequency ω_r greater than the proton cyclotron frequency, whereas the electron mirror instability is excited at propagation oblique to $\mathbf{B}_o$ and zero real frequency. In an unmagnetized plasma the electron Weibel instability may be excited under the same conditions with zero real frequency and maximum growth rate in the direction of the minimum temperature. Here linear theory is used to compare dispersion and threshold properties of these three growing modes. For $0.10 \leq \beta_{\parallel e} \leq 1000$, the whistler has a larger γ_m and a smaller anisotropy threshold than the electron mirror, so that the former mode should dominate in homogeneous plasmas for most physical values of electron β. Threshold conditions describing electron temperature anisotropies and parallel wavenumbers at given maximum growth rates are presented for each instability.

I. Introduction

The collisionless tearing instability is often regarded as the primary large-scale manifestation of reconnection at the Earth's magnetopause and in the terrestrial magnetotail. Theory predicts that this instability is a sensitive function of the electron temperature

anisotropy (e.g. *Karimabadi et al.*, 2004, 2005, and references therein), with $T_{\perp e}/T_{\parallel e} > 1$ yielding a substantial enhancement of this growth rate (The various symbols used here are defined in the Appendix.). Recent computer simulations of the tearing mode [*Ricci et al.*, 2004] have confirmed this prediction, suggesting that $T_{\perp e}/T_{\parallel e}$ is a critical parameter for determining the onset and saturation of collisionless reconnection.

A possible source of electron anisotropy in a reconnection configuration has been demonstrated by *Daughton et al.* [2004]. Their particle-in-cell simulations of a current sheet in a collisionless plasma have demonstrated that the growth of the lower hybrid drift instability heats electrons in the directions perpendicular to the magnetic field. On the other hand, electron temperature anisotropies are limited in magnitude; theory and simulations of uniform magnetized plasmas have shown that the whistler anisotropy instability scatters electrons so as to impose a β_e-dependent upper bound on $T_{\perp e}/T_{\parallel e}$ (*Gary and Wang*, 1996; *Gary et al.*, 2000; *Nishimura et al.*, 2002) and recent observations demonstrate that this theoretical constraint is satisfied in the terrestrial magnetosheath (*Gary et al.*, 2005). These considerations imply that, to provide the proper context for application of electron temperature anisotropies to the tearing instability, it is appropriate to re-examine and compare the linear theory properties of the various short wavelength resonant instabilities driven by this electron anisotropy.

In a magnetized plasma there are two distinct electromagnetic instabilities driven by $T_{\perp e}/T_{\parallel e} > 1$ (Here e denotes electrons and the other subscripts indicate directions relative to the background magnetic field $\mathbf{B}_o$.). The whistler anisotropy instability has been studied extensively through both linear theory [*Kennel and Petschek*, 1966; *Scharer and Trivelpiece*, 1967; *Gary*, 1993] and computer simulation [*Ossakow et al.*, 1972; *Cuperman*, 1981; *Pritchett et al.*, 1991; *Devine et al.*, 1995; *Gary and Wang*, 1996; *Nishimura et al.*, 2002]. The electron mirror instability has received less scrutiny [*Pokhotelov et al.*, 2002]; its name derives from the many properties it shares with the better-known ion mirror instability driven by an ion $T_\perp > T_\parallel$. These common properties include $\omega_r = 0$ in a homogeneous plasma, maximum growth rate at propagation oblique to $\mathbf{B}_o$, predominantly compressive, that is, $|\delta B_\parallel|^2 >> |\delta B_\perp|^2$, and the Landau resonance of the anisotropic species as the primary driver of the instability.

Electromagnetic growing modes driven by electron temperature anisotropies in an unmagnetized plasma are known as "Weibel instabilities" [*Weibel*, 1959]. For fluctuations at $\mathbf{k} = \hat{\mathbf{z}}k$ and electron temperatures $T_x = T_y = T_\perp > T_z = T_\parallel$ linear theory predicts [*Kalman*

Table 1. Electromagnetic instabilities driven by $T_{\perp e}/T_{\parallel e} > 1$

Instability	Magnetic field	Real frequency	Wavevector at γ_m	
Whistler anisotropy	$\mathbf{B}_o \neq 0$	$\Omega_i < \omega_r < \lvert\Omega_e\rvert$	$k_m c/\omega_e < 1$	$\theta = 0^o$
Electron mirror	$\mathbf{B}_o \neq 0$	$\omega_r = 0$	$k_m c/\omega_e < 1$	$\theta \neq 0^o$
Electron Weibel	$\mathbf{B}_o = 0$	$\omega_r = 0$	$k_m c/\omega_e < 1$	$\theta = 0^o$

et al., 1968; *Yoon*, 1989], and nonlinear theory [*Montes and Winske*, 1970; *Lemons and Winske*, 1980] and computer simulations [*Morse and Nielson*, 1971; *Lemons et al.*, 1979] are consistent with, an electron Weibel instability with $\omega_r = 0$ and propagation parallel to the $\hat{\mathbf{z}}$ direction. Table 1 summarizes selected properties of these three electromagnetic instabilities.

Here linear theory is used to compare dispersion and threshold properties of these three instabilities. All results presented here are derived from the linear dispersion equation in a homogeneous, collisionless plasma. If the background magnetic field is nonzero, the general form of this equation at $\mathbf{k} \times \mathbf{B}_o = 0$ is

$$\omega^2 - k^2c^2 + k^2c^2 \sum_j S_j^{\pm}(\mathbf{k}, \omega) = 0$$

If the velocity distribution of each species j is represented as a single anisotropic bi-Maxwellian, it follows that [e.g., *Gary*, 1993]

$$S_j^{\pm}(\mathbf{k}, \omega) = \frac{\omega_j^2}{k^2c^2} \left[\zeta_j Z(\zeta_j^{\pm}) + \left(1 - \frac{T_{\perp j}}{T_{\parallel j}}\right) \frac{Z'(\zeta_j^{\pm})}{2} \right]$$

In the limit of $B_o = 0$, the dimensionless conductivity becomes

$$S_j(\mathbf{k}, \omega) = \frac{\omega_j^2}{k^2c^2} \left[\zeta_j Z(\zeta_j) + \left(1 - \frac{T_{\perp j}}{T_{\parallel j}}\right) \frac{Z'(\zeta_j)}{2} \right]$$

We consider two species: ions (denoted by subscript i) and electrons. We assume that the average relative drift between the electrons and ions is zero, and that charge neutrality $n_e = n_i$ holds. We assume the following dimensionless parameters: $m_i/m_e = 1836$, $T_{\parallel e}/T_{\parallel i} = 1$ and, to isolate the consequences of the electron anisotropy, $T_{\perp i}/T_{\parallel i} = 1$.

II. Dispersion

Solutions of the linear dispersion equation for a collisionless plasma are typically expressed in terms of dimensionless variables. For the electron Weibel instability, it is natural to use the electron inertial length and the electron plasma frequency as normalizing factors; thus our results for this growing mode are described in terms of kc/ω_e and γ/ω_e. Then the dimensionless parameter which characterizes the electron temperature is $k_B T_{\|e}/mc^2$.

For the whistler anisotropy and electron mirror instabilities, kc/ω_e is again an appropriate dimensionless variable, but frequencies and growth rates are usually normalized by the electron cyclotron frequency. In this case, the electron temperature is characterized by $\beta_{\|e}$, and dimensionless frequencies, growth rates, and wavenumbers are essentially independent of $\omega_e/|\Omega_e|$ as long as this parameter is substantially greater than unity. For comparison of these two magnetized instabilities, these normalizations are the natural ones to use. However, to compare all three instabilities, it is necessary to make the complex frequency dimensionless by dividing by ω_e. Then scaling relations for the magnetized instabilities should be constructed by varying both $\beta_{\|e}$ and $\omega_e/|\Omega_e|$ so that $k_B T_{\|e}/mc^2$ remains constant.

Figure 1 compares the $\gamma(k)$ for the three instabilities. Here and for a broad range of parameters the following ordering obtains:

$$\gamma_m(\text{Electron mirror}) < \gamma_m(\text{Whistler anisotropy}) \leq \gamma_m(\text{Electron Weibel})$$

Given that $\omega_r = 0$ for both the mirror and Wiebel instabilities, one might expect that these two modes would display similar $\gamma(k)$. But Figure 1 shows this is not the case; it is the $\gamma(k_\|)$ of the whistler which closely resembles the Weibel growth rate.

Figure 2 illustrates the growth rate maximized with respect to wavenumber and the corresponding wavenumber as a function of θ for the two modes in a magnetized plasma. This shows that $\gamma(\mathbf{k})$ lies at $\mathbf{k} \times \mathbf{B}_o = 0$ for the whistler and at $\theta \neq 0$ for the electron mirror instability.

III. Threshold Conditions

This section describes several threshold conditions for linear theory thresholds of electron temperature anisotropy instabilities. We derive these threshold conditions in magnetized plasmas as follows. We first choose a value for the maximum dimensionless

growth rate, e.g., $\gamma_m/|\Omega_e| = 0.01$. We next numerically solve the full linear dispersion equation for many values of $\beta_{\parallel e}$, obtaining the corresponding frequency, growth rate, and wavevector for both the whistler anisotropy and the electron mirror instabilities. We find that both the parallel wavenumber at maximum growth rate $k_{\parallel m}$ and the electron anisotropy $T_{\perp e}/T_{\parallel e}$ are monotonically decreasing functions of $\beta_{\parallel e}$ for both growing modes. Third, we carry out least-squares fits of the wavenumber and the anisotropy as functions of $\beta_{\parallel e}$ over limited ranges of the latter parameter.

Gary and Wang (1996) showed that the linear theory threshold condition for the whistler anisotropy instability can be written as

$$\frac{T_{\perp e}}{T_{\parallel e}} - 1 = \frac{S_e}{\beta_{\parallel e}^{\alpha_e}} \tag{1}$$

where the fitting parameters S_e and α_e are functions of the choice of maximum growth rate and the range of $\beta_{\parallel e}$ values over which the fit is carried out. Figure 3(a) shows that the anisotropy threshold condition for both instabilities can be well fit to Equation (1) over $10 \leq \beta_{\parallel e} \leq 1000$ at $\gamma_m/|\Omega_e| = 0.01$; Table 2 states the associated fitting parameters for three different values of the maximum growth rate. Figure 3(a) shows that the electron mirror instability threshold anisotropy is substantially higher than that of the cyclotron-resonant whistler anisotropy instability for $0.10 \leq \beta_{\parallel e} \leq 1000$. We conclude that the latter mode should be the dominant electron temperature anisotropy instability for virtually all physical values of electron β, and the absence of space plasma observations of the electron mirror mode supports this conclusion.

It is instructive to compare these results to the threshold conditions of two electromagnetic instabilities driven by the proton anisotropy $T_\perp/T_\parallel > 1$. Such conditions for both the proton cyclotron anisotropy instability and the proton mirror instability also satisfy Equation (1) with subscripts p substituted for subscripts e. A major difference between the two pairs of modes, however, is that the threshold curves of the two proton anisotropy instabilities cross at $\beta_{\parallel p} \simeq 7$ [*Gary et al.*, 1994], so that the proton mirror mode has the faster growth rate and is likely to be the more important source of enhanced fluctuations at this and larger values of $\beta_{\parallel p}$. This conclusion is supported by a number of space plasma observations of enhanced proton mirror fluctuations in the magnetosheath [e.g. *Anderson et al.*, 1994] as well as more indirect evidence for the excitation of the proton mirror mode in the solar wind [*Winterhalter et al.*, 1994].

A second expression which emerges from linear dispersion theory describes the par-

Table 2. Fitting Parameters to Threshold Conditions:

Whistler Anisotropy Instability

$10 \leq \beta_{\|e} \leq 1000$

$\gamma_m/\|\Omega_e\|$	S_k	α_k	S_e	α_e
0.001	0.36	0.33	0.15	0.55
0.01	0.40	0.26	0.25	0.43
0.10	0.56	0.20	0.80	0.37

Electron Mirror Instability

$10 \leq \beta_{\|e} \leq 1000$

$\gamma_m/\|\Omega_e\|$	S_k	α_k	S_e	α_e
0.001	0.048	0.13	0.53	0.64
0.01	0.114	0.12	0.74	0.50
0.10	0.27	0.11	2.21	0.46

allel wavenumber at instability threshold:

$$\frac{k_{\|}c}{\omega_e} = \frac{S_k}{\beta_{\|e}^{\alpha_k}} \tag{2}$$

where the fitting parameters S_k and α_k are functions of the choice of maximum growth rate and the range of $\beta_{\|e}$ values over which the fit is carried out. Figure 3(a) shows that the wavenumber threshold condition for both instabilities can be well fit to Equation (2) over $10 \leq \beta_{\|e} \leq 1000$ at $\gamma_m/|\Omega_e| = 0.01$; Table 2 states the fitting parameters to Equation (2) for three different values of the maximum growth rate.

The implication of Figure 3(b) and Table 2 is that the parallel wavenumber of the electron mirror instability at a given threshold is universally smaller than the same quantity at threshold of the whistler anisotropy instability. Furthermore, Figure 1 suggests, and sample computations not described here confirm, that for a broad range of plasma parameters

$$k_{\|m}(\text{Electron mirror}) < k_{\|m}(\text{Electron Weibel}) \leq k_{\|m}(\text{Whistler anisotropy})$$

A third threshold condition is related to the oft-quoted relationship for the electron Weibel instability $T_{\perp e}/T_{\parallel e} - 1 = (kc/\omega_e)^2$ [*Lemons et al.*, 1979; *Yoon*, 1989] which represents the maximum wavenumber available to growing fluctuations. Figure 1 suggests that this relationship also applies to the whistler anisotropy instability. Solutions of the linear dispersion equation yield what may be an even more useful threshold condition for the electron Weibel instability:

$$\frac{T_{\perp e}}{T_{\parallel e}} - 1 = 3\left(\frac{k_m c}{\omega_e}\right)^2 \tag{3}$$

for $k_m c/\omega_e << 1$. Further, we find this result to be independent of the value of $k_B T_{\parallel e}/m_e c^2$. Figure 4 illustrates this result and, furthermore, shows that it is approximately true for an intermediate range of wavenumbers for the whistler anisotropy instability. At the relatively long wavelengths corresponding to weak anisotropies, ion cyclotron damping quenches the whistler anisotropy instability and Equation (3) is no longer appropriate for that growing mode.

IV. Conclusions

We used linear theory to compare the properties of three growing modes excited by $T_{\perp e}/T_{\parallel e} > 1$: the whistler anisotropy instability and the electron mirror instability in a magnetized plasma and the electron Weibel instability in an unmagnetized plasma. Over $0.10 \leq \beta_{\parallel e} \leq 1000$ the first two of these modes have anisotropy thresholds with the form of Equation (1), although the whistler instability has the uniformly lower threshold. Similarly, the electron Weibel and whistler anisotropy instabilities satisfy the threshold condition Equation (3).

The threshold conditions described here may be useful proxies for describing the consequences of scattering by the relatively short wavelength modes studied here. For example, if a plasma is magnetized with relatively weak gradients parallel to $\mathbf{B}_o$, as may be the case in a plasma sheet with a so-called guide magnetic field, then the whistler will be the most important growing mode driven by this electron anisotropy. Particle-in-cell simulations have shown that this instability growth leads to electron scattering; a consequence of this scattering is to reduce the electron temperature anisotropy to or below the instability threshold condition. Then Equation (1) with fitting parameters corresponding to an appropriate instability growth rate determines the maximum anisotropy which can be sustained under such conditions. Under the plausible assumption that instability growth and scattering rates are much faster than the growth rate of a large-scale instability such

as the tearing mode, Equation (1) then provides an upper bound on the $T_{\perp e}/T_{\parallel e}$ which, in turn, provides a limit on the tearing growth rate.

Appendix

For the jth species we define $\beta_{\parallel j} \equiv 8\pi n_j k_B T_{\parallel j}/B_o^2$; the plasma frequency, $\omega_j \equiv \sqrt{4\pi n_j e_j^2/m_j}$; the cyclotron frequency, $\Omega_j \equiv e_j B_o/m_j c$; and the thermal speed, $v_j \equiv \sqrt{k_B T_{\parallel j}/m_j}$. The Alfvén speed is $v_A \equiv B_o/\sqrt{4\pi n_i m_i}$. The complex frequency is $\omega = \omega_r + i\gamma$, the Landau resonance factor of the jth species is $\zeta_j \equiv \omega/\sqrt{2}|k_\parallel|v_j$, and the cyclotron resonance factors of the jth species are $\zeta_j^\pm \equiv (\omega \pm \Omega_j)/\sqrt{2}|k_\parallel|v_j$. The choice of coordinate system is such that both $\mathbf{B}_o$ and the wavevector $\mathbf{k}$ lie in the y-z plane. We define θ as the angle between $\mathbf{k}$ and $\mathbf{B}_o$, so that $\hat{\mathbf{k}} \cdot \hat{\mathbf{B}}_o = \cos(\theta)$. Subscript m denotes a quantity corresponding to the maximum growth rate γ_m/Ω_i; thus k_m and θ_m correspond to the wavevector which yields the largest value of γ for a given set of dimensionless plasma parameters.

Acknowledgments. This work was performed at Los Alamos National Laboratory under the auspices of the U.S. Department of Energy (DOE) and was supported by the DOE Office of Basic Energy Sciences, Division of Engineering and Geosciences, and the Sun-Earth Connection Theory Program of the National Aeronautics and Space Administration.

References

Anderson, B. J., S. A. Fuselier, S. P. Gary, and R. E. Denton (1994), Magnetic spectral signatures in the Earth's magnetosheath and plasma depletion layer, *J. Geophys. Res.*, *99*, 5877.

Cuperman, S. (1981), Electromagnetic kinetic instabilities in multicomponent space plasmas: Theoretical predictions and computer simulation experiments, *Revs. Geophys. Space Phys.*, *19*, 307.

Daughton, W., G. Lapenta, and P. Ricci (2004), Nonlinear evolution of the lower-hybrid drift instability in a current sheet, *Phys. Rev. Lett.*, *93*, 105004.

Devine, P. E., S. C. Chapman, and J. W. Eastwood (1995), One- and two-dimensional simulations of whistler mode waves in an anisotropic plasma, *J. Geophys. Res.*, *100*, 17,189.

Gary, S. P. (1993), *Theory of Space Plasma Microinstabilities*, Cambridge Univ. Press, New York.

Gary, S. P., and J. Wang (1996), Whistler instability: electron anisotropy upper bound, *J. Geophys. Res.*, *101*, 10,749.

Gary, S. P., B. J. Anderson, R. E. Denton, S. A. Fuselier, and M. E. McKean (1994), A limited closure relation for anisotropic plasmas from the Earth's magnetosheath, *Phys. Plasmas*, *1*, 1676.

Gary, S. P., D. Winske, and M. Hesse (2000), Electron temperature anisotropy instabilities: Computer simulations, *J. Geophys. Res.*, *105*, 10,751.

Gary, S. P., B. Lavraud, M. F. Thomsen, B. Lefebvre, and S. J. Schwartz (2005), Electron anisotropy constraint in the magnetosheath: Cluster observations, *Geophys. Res. Lett.*, *32*, L13109, doi:10.1029/2005GL023234.

Kalman, G., C. Montes, and D. Quemada (1968), Anisotropic temperature plasma instabilities, *Phys. Fluids*, *11*, 1797.

Karimabadi, H., W. Daughton, and K. B. Quest (2004), Role of electron temperature anisotropy in the onset of magnetic reconnection, *Geophys. Res. Lett.*, *31*, L18801, doi:10.1029/2004GL020791.

Karimabadi, H., W. Daughton, and K. B. Quest (2005), Physics of saturation of collisionless tearing mode as a function of guide field, *J. Geophys. Res.*, *110*, A03214, doi:10.1029/2004JA010749.

Kennel, C. F., and H. E. Petschek (1996), Limit on stably trapped particle fluxes, *J. Geophys. Res.*, *71*, 1.

Lemons, D. S., D. Winske, and S. P. Gary (1979), Nonlinear theory of the Weibel instability, *J. Plasma Phys.*, *21*, 287.

Lemons, D. S., and D. Winske (1980), Statistical thermodynamics of temperature anisotropy driven Weibel instabilities, *J. Plasma Phys.*, *23*, 283.

Montes, C., J. Coste, and G. Diener (1970), Relaxation of a temperature anisotropy in a collisionless plasma, *J. Plasma Phys.*, *4*, 21.

Morse, R. L., and C. W. Nielson (1971), Numerical simulation of the Weibel instability in one and two dimensions, *Phys. Fluids*, *14*, 830.

Nishimura, K., S. P. Gary, and H. Li (2002), whistler anisotropy instability: Wave-particle scattering rate, *J. Geophys. Res.*, *107*, 1375, doi:10.1029/2002JA009250.

Ossakow, S. L., I. Haber, and E. Ott (1972), Simulation of whistler instabilities in anisotropic plasmas, *Phys. Fluids*, *15*, 1538.

Pokhotelov, O. A., r. A. Treumann, R. Z. Sagdeev, M. A. Balikhin, O. G. On-

ishchenko, V. P. Pavlenko, and I. Sandberg (2002), Linear theory of the mirror instability in non-Maxwellian space plasmas, *J. Geophys. Res.*, *107*, 1312, doi:10.1029/2001JA009125.

Pritchett, P. L., D. Schriver, and M. Ashour-Abdalla (1991), Simulation of whistler waves excited in the presence of a cold plasma cloud: Implications for the CRRES mission, *J. Geophys. Res.*, *96*, 19,507.

Ricci, P., J. U. Brackbill, W. Daughton, and G. Lapenta (2004), New role of the lower hybrid drift instability in the magnetic reconnection, *Phys. Plasmas*, *12*, 055901.

Scharer, J. E., and A. W. Trivelpiece (1967), Cyclotron wave instabilities in a plasma, *Phys. Fluids*, *10*, 591.

Weibel, E. S. (1959), Spontaneously growing transverse waves in a plasma due to an anisotropic velocity distribution, *Phys. Rev. Lett.*, *2*, 83.

Winterhalter, D., M. Neugebauer, B. E. Goldstein, E. J. Smith, S. J. Bame, and A. Balogh (1994), Ulysses field and plasma observations of magnetic holes in the solar wind and their relation to mirror-mode structures, *J. Geophys. Res.*, *99*, 23,371.

Yoon, P. H. (1989), Electromagnetic Weibel instability in a fully relativistic bi-Maxwellian plasma, *Phys. Fluids*, *B 1*, 1336.

Figure Captions

Figure 1. Growth rates of three electron temperature anisotropy instabilities at θ values corresponding to γ_m as functions of the fluctuation wavenumber. Results for the whistler anisotropy instability are at $\mathbf{k} \times \mathbf{B}_o = 0$ and are indicated by solid dots. Results for the electron mirror instability are at $\theta_m = 52^o$ and are indicated by open circles. Results for the electron Weibel instability are at $\mathbf{k} = \hat{\mathbf{z}}k$ and are shown as crosses. Here $k_B T_{\|e}/m_e c^2 = 10^{-3}$, and $T_{\perp e}/T_{\|e} = 1.10$. For the modes in a magnetized plasma, $\omega_e/|\Omega_e| = 223.57$, which implies $\beta_{\|e} = 100.0$.

Figure 2. (a) The growth rates maximized over wavenumber at fixed θ and (b) the corresponding wavenumbers as functions of the direction of propagation for the whistler anisotropy and electron mirror instabilities. Here $\omega_e/|\Omega_e| = 223.57$, $\beta_{\|e} = 100.0$ and $T_{\perp e}/T_{\|e} = 1.10$.

Figure 3. (a) Electron temperature anisotropy and (b) parallel dimensionless wavenumber at the $\gamma_m/|\Omega_e| = 0.01$ thresholds of two instabilities as functions of $\beta_{\|e}$. In each case the discrete symbols represent linear theory results; the lines are least-squares fits to these points over $10 \leq \beta_{\|e} \leq 1000$. The solid symbols and the solid lines correspond

to the whistler anisotropy instability; the open symbols and the dashed lines represent the electron mirror instability. Here $\omega_e/|\Omega_e| = 223.57$.

Figure 4. The electron temperature anisotropy at maximum growth rate as a function of the square of the wavenumber at maximum growth rate. The solid dots represent results for the whistler anisotropy instability, whereas the crosses represent results for the electron Weibel instability. The dashed line represents Equation (3). Here $k_B T_{\|e}/m_e c^2 = 10^{-3}$. For the whistler $\omega_e/|\Omega_e| = 223.57$, which implies $\beta_{\|e} = 100.0$.

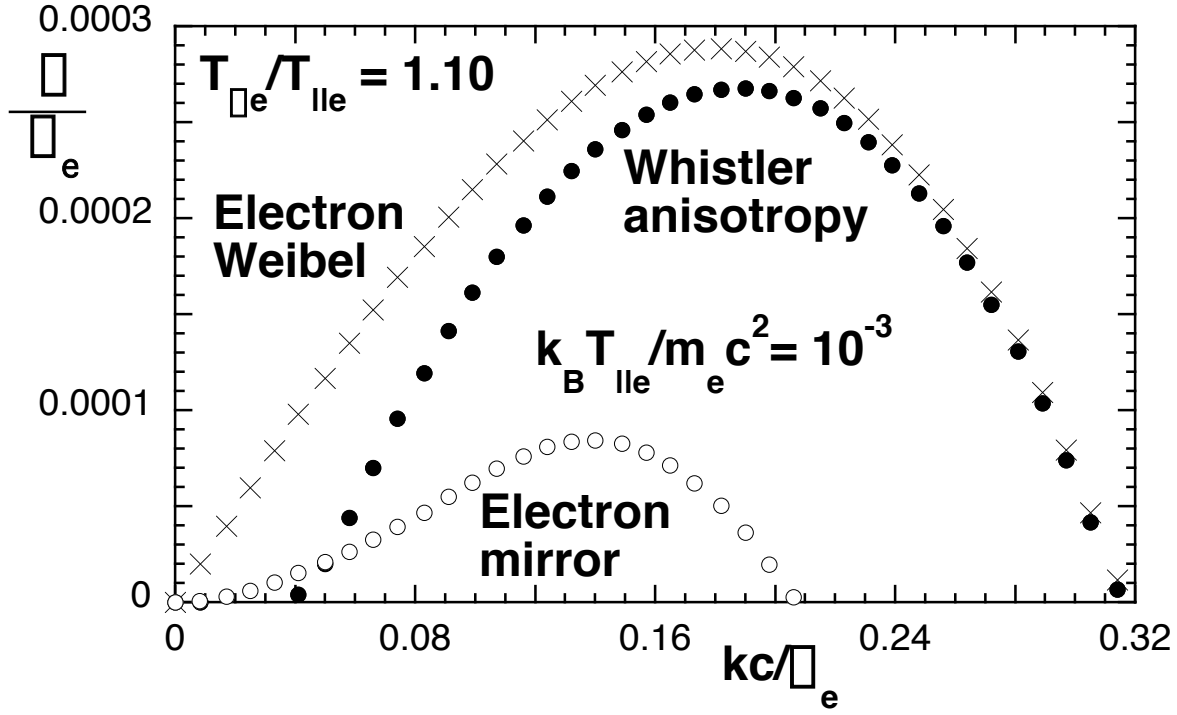
0.0003
0.0002
0.0001
0
0
0.08
0.16
0.24
0.32
T⊥e/Tlle = 1.10
Whistler
anisotropy
Electron
Weibel
kBTlle/mec2= 10-3
Electron
mirror
kc/ωe

Figure 1

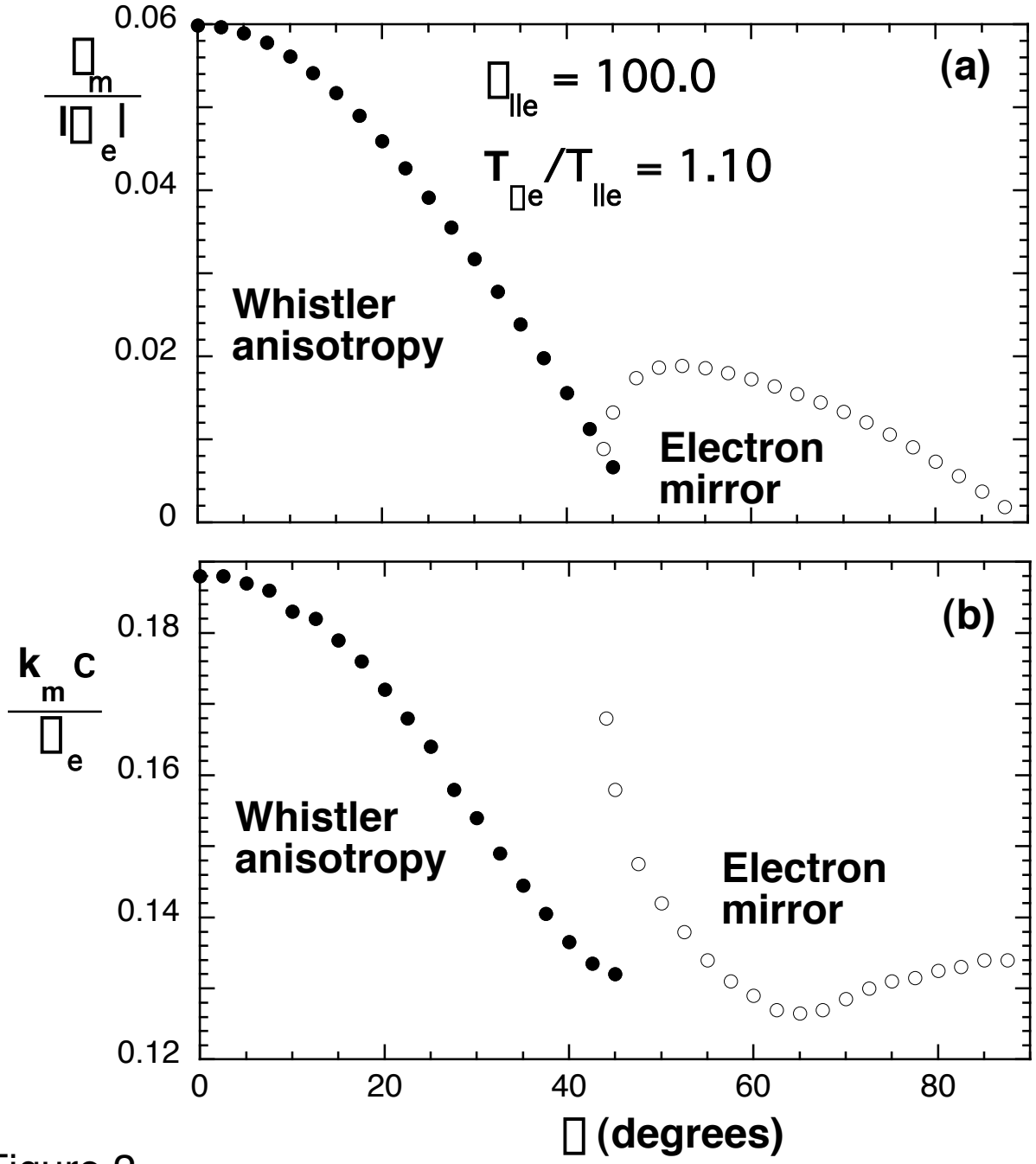
0.06
0.04
0.02
0
(a)
Whistler
anisotropy
Electron
mirror
0.18
0.16
0.14
0.12
(b)
Whistler
anisotropy
Electron
mirror
0
20
40
60
80
(degrees)

Figure 2

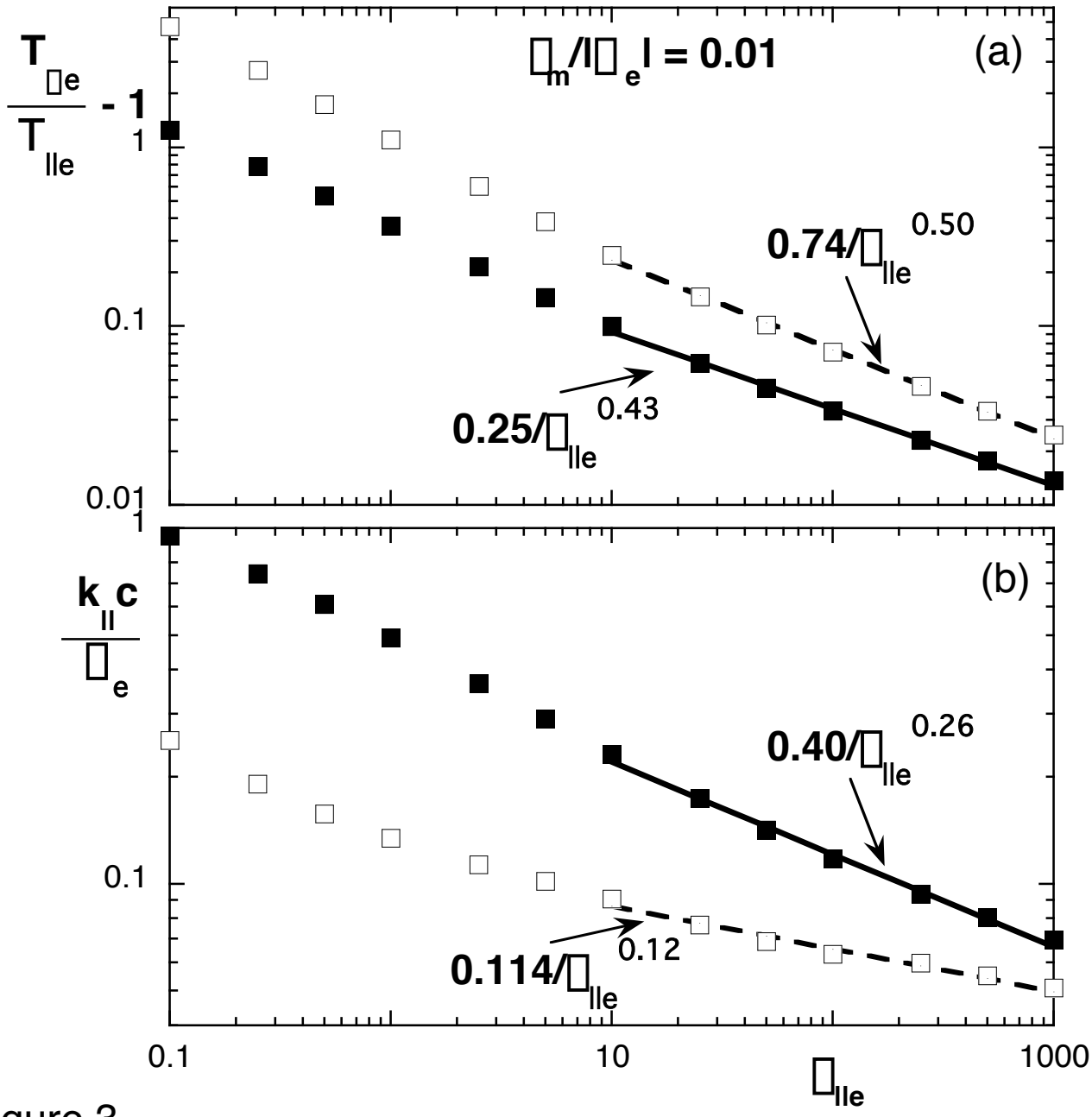
$\frac{T_{\perp e}}{T_{\parallel e}} - 1$
$\omega_m/|\omega_e| = 0.01$
(a)
1
0.1
0.01
0.74/$\Omega_{\parallel e}$
0.50
0.25/$\Omega_{\parallel e}$
0.43
$\frac{k_\parallel c}{\omega_e}$
(b)
0.40/$\Omega_{\parallel e}$
0.26
0.114/$\Omega_{\parallel e}$
0.12
0.1
10
1000
$\Omega_{\parallel e}$

Figure 3

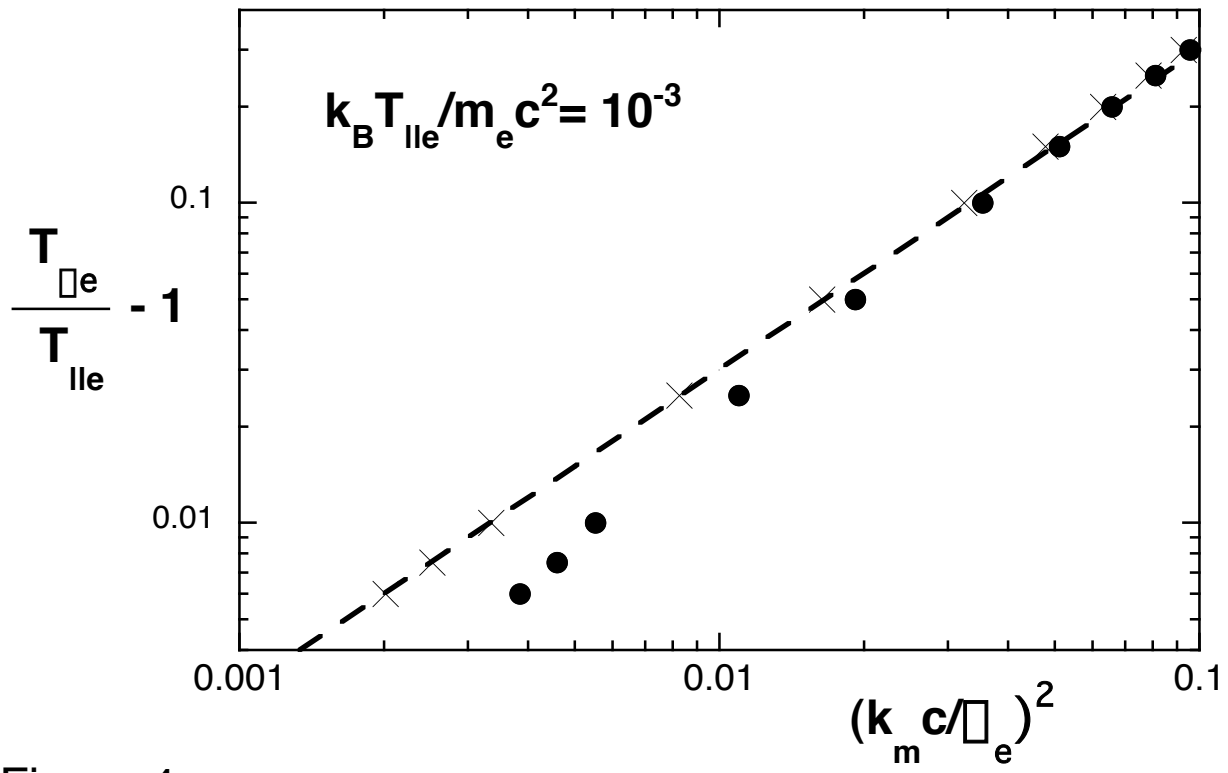
$k_B T_{lle}/m_e c^2 = 10^{-3}$
$\frac{T_{\parallel e}}{T_{lle}} - 1$
0.1
0.01
0.001
0.01
0.1
$(k_m c/\omega_e)^2$

Figure 4